electronic reprint

STRUCTURAL CHEMISTRY

ISSN: 2053-2296

journals.iucr.org/c

Invariom-model refinement and Hirshfeld surface analysis of well-ordered solvent-free dibenzo-21-crown-7

Dennis Wiedemann and Julia Kohl

Acta Cryst. (2017). C**73**, 654–659

Acta Cryst C STRUCTURAL CHEMISTRY
ISSN 2053-2296

Invariom-model refinement and Hirshfeld surface analysis of well-ordered solvent-free dibenzo-21-crown-7

Dennis Wiedemann* and Julia Kohl

Institut für Chemie, Technische Universität Berlin, Strasse des 17 Juni 135, 10623 Berlin, Germany. *Correspondence e-mail: dennis.wiedemann@chem.tu-berlin.de

Received 13 July 2017
Accepted 27 July 2017

Edited by A. L. Spek, Utrecht University, The Netherlands

Keywords: crown ethers; crystal structure; invariom refinement; intermolecular interactions; Hirshfeld surface; interaction energies.

CCDC references: 1565414; 1565413

Supporting information: this article has supporting information at journals.iucr.org/c

Crown ethers and their supramolecular derivatives are well-known chelators and scavengers for a variety of cations, most notably heavier alkali and alkaline-earth ions. Although they are widely used in synthetic chemistry, available crystal structures of uncoordinated and solvent-free crown ethers regularly suffer from disorder. In this study, we present the X-ray crystal structure analysis of well-ordered solvent-free crystals of dibenzo-21-crown-7 (systematic name: dibenzo[*b*,*k*]-1,4,7,10,13,16,19-heptaoxacycloheneicosa-2,11-diene, $C_{22}H_{28}O_7$). Because of the quality of the crystal and diffraction data, we have chosen invariom, in addition to standard independent spherical atoms, for modelling and briefly discuss the different refinement results. The electrostatic potential, which is directly deducible from the invariom model, and the Hirshfeld surface are analysed and complemented with interaction-energy computations to characterize intermolecular contacts. The boat-like molecules stack along the *a* axis and are arranged as dimers of chains, which assemble as rows to form a three-dimensional structure. Dispersive C—H···H—C and C—H···π interactions dominate, but nonclassical hydrogen bonds are present and reflect the overall rather weak electrostatic influence. A fingerprint plot of the Hirshfeld surface summarizes and visualizes the intermolecular interactions. The insight gained into the crystal structure of dibenzo-21-crown-7 not only demonstrates the power of invariom refinement, Hirshfeld surface analysis and interaction-energy computation, but also hints at favourable conditions for crystallizing solvent-free crown ethers.

1. Introduction

Macrocyclic crown ethers are established chelators particularly suited for substituted ammonium ions and heavy-metal cations (Pedersen, 1967). The title compound, dibenzo-21-crown-7 (systematic name: dibenzo[*b*,*k*]-1,4,7,10,13,16,19-heptaoxacycloheneicosa-2,11-diene, also 6,7,9,10,12,13,20,21,-23,24-decahydrodibenzo[*b*,*k*][1,4,7,10,13,16,19]heptaoxacycloheneicosin; Chemical Abstracts Service, 2017), (I), is known to selectively form stable complexes with ions of heavy alkali and alkaline-earth metals, most notably caesium (Blasius & Nilles, 1984).

Although Petersen had synthesized the molecule in the late 1960s, the first reliable crystal structure of the nitromethane adduct of (I) was not established until the mid-1990s (Burns *et al.*, 1996). Only three closely related derivatives, namely dimethyldibenzo-21-crown-7 (Owen & Nowell, 1978), 4,4′-di-*tert*-octyldibenzo-21-crown-7 (Sachleben *et al.*, 1997) and tetranitrodibenzo-21-crown-7 (Mäkelä *et al.*, 2016), have been characterized using X-ray diffraction, probably because of the notorious tendency of crown ethers to disorder, especially when uncoordinated.

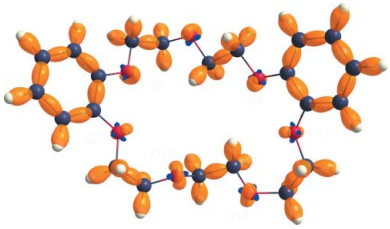

Table 1
Experimental details.

Chemical formula = $C_{22}H_{28}O_7$, M_r = 404.44, crystal system = monoclinic, space group = $P2_1/c$ and Z = 4. The experiment was carried out at 150.00 (10) K with Cu $K\alpha$ radiation using an Agilent SuperNova (single source) diffractometer. Absorption was corrected for using numerical methods based on Gaussian integration over a 14-faceted crystal model (grid dimensions: 10^3, beam-profile correction for 0.18 × 0.18 mm^2). An empirical absorption correction was then performed using spherical harmonics and frame scaling (minimum factor: 0.662; maximum factor: 1.465), as implemented in *CrysAlis PRO* (Rigaku Oxford Diffraction, 2015).

	IAM	Invariom model
Crystal data		
a, b, c (Å)	4.9801 (1), 17.4771 (2), 23.1000 (2)	
β (°)	94.124 (1)	
V (Å^3)	2005.37 (5)	
μ (mm^{-1})	0.82	
Crystal size (mm)	0.74 × 0.14 × 0.08	
Data collection		
T_{min}, T_{max}	0.598, 1.000	
No. of measured, independent and observed [$I > 2\sigma(I)$] reflections	13236, 3925, 3559	
R_{int}	0.018	
(sin $\theta/\lambda)_{max}$ (Å^{-1})	0.622	
Refinement		
$R[F^2 > 2\sigma(F^2)]$, $wR(F^2)$, S	0.038, 0.103, 1.05	0.030, 0.084, 0.98
No. of reflections	3925	3664
No. of parameters	262	290
H-atom treatment	H-atom parameters constrained	Only H-atom displacement parameters refined
Weighting scheme	$w = 1/[\sigma^2(F_o^2) + (0.0497P)^2 + 0.7337P]$ where $P = (F_o^2 + 2F_c^2)/3$	$w = 1/[\sigma^2(F_o^2) + (0.0497P)^2 + 0.1P]$ where $P = (F_o^2 + 2F_c^2)/3$
$\Delta\rho_{max}$, $\Delta\rho_{min}$, r.m.s. $\Delta\rho$ (e Å^{-3})	0.39, −0.28, 0.04	0.41, −0.24, 0.03

Computer programs: *CrysAlis PRO* (Rigaku Oxford Diffraction, 2015), *SHELXT* (Sheldrick, 2015*a*), *SHELXL2016* (Sheldrick, 2015*b*), *XD2016* (Volkov *et al.*, 2016), *ORTEP-3 for Windows* (Farrugia, 2012), *Mercury* (Macrae *et al.*, 2008), *OLEX2* (Dolomanov *et al.*, 2009) and *WinXD* (Volkov *et al.*, 2016).

In this article, we present the crystal structure of well-ordered solvent-free dibenzo-21-crown-7. Inspired by a talk given by K. Woźniak (Sanjuan-Szklarz *et al.*, 2016) and because of the suitability of our data set, we go beyond the

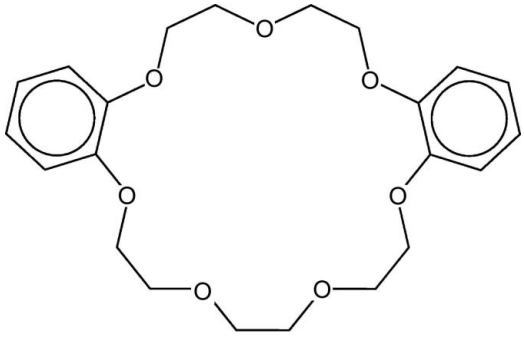

(I)

spherical independent atom model (IAM), which is the standard in crystal structure modelling. For the purpose of full characterization, we also apply the invariom approach, which assigns an aspherical atomic form factor to each atom according to its nature and chemical environment (Dittrich *et al.*, 2004).

2. Experimental

2.1. Crystallization

Dibenzo-21-crown-7 (98%) and toluene were purchased from Acros Organics. The crown ether was dried *in vacuo* overnight. The solvent was distilled over sodium benzophenone ketyl and stored over molecular sieves (4 Å) before use.

In a Schlenk tube, a sample of (I) was dissolved in toluene (5 ml). The Schlenk tube was then connected to a second empty such tube *via* a curved glass connector. The solution was frozen by immersing the first tube in liquid nitrogen, and the whole apparatus was evacuated to *ca* 10^{-2} hPa. The frozen solution was then allowed to warm to room temperature (*ca* 293 K) and the empty Schlenk tube was dipped into a Dewar vessel containing slightly cooler water (*ca* 291 K). The small temperature gradient allowed the toluene to evaporate slowly from the solution, resulting in the growth of colourless single crystals suitable for diffractometry within five days. We were satisfied with obtaining crystals under these special conditions and did not further optimize the crystal size with respect to suitability for the micro-focus source.

2.2. Refinement

Crystal data, data collection and structure refinement details are summarized in Table 1. Firstly, a conventional IAM refinement was performed using *SHELXL2016* (Sheldrick, 2015*b*) with *OLEX2* (Dolomanov *et al.*, 2009) as a front end. All H atoms were located in difference Fourier maps and constrained using a standard riding model, with C—H = 0.99 Å for methylene groups and 0.95 Å for aromatic groups, and with U_{iso}(H) = 1.2U_{eq}(C).

Based on the refined IAM, *MoleCoolQt* (Hübschle & Dittrich, 2011) was used to assign and check invariom and

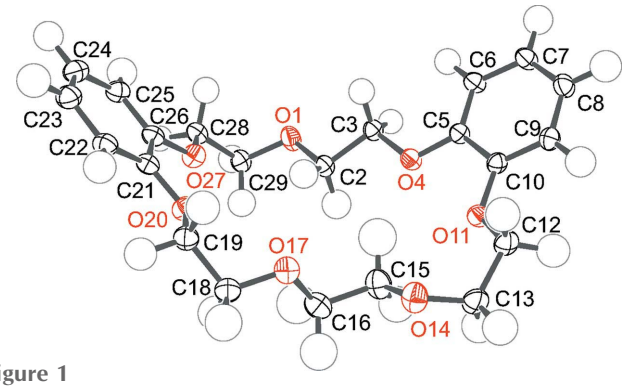

Figure 1
An *ORTEP* representation, with displacement ellipsoids and spheres drawn at the 50% probability level, of the molecular structure of (I) according to the invariom model (colour key: C atoms black, O atoms red and H atoms grey).

local coordinate systems, import them from the generalized invariom database (Dittrich *et al.*, 2013) and set up input files for the next step (*cf.* Table S1 in the supporting information). The resulting model, which is based on multipoles according to the Hansen–Coppens formalism (Hansen & Coppens, 1978), was then refined with *XD2016* (Volkov *et al.*, 2016) against a data set merged using tools implemented in *WinGX* (Farrugia, 2012). To assure comparability of weighted results, the limit for observed reflections was lowered to $I > 2\sigma(I)$ and a *SHELXL*-like weighting scheme with $a(XD) = p(SHELXL)$ and $b(XD) = 0.1$ was applied, so that the weighted goodness-of-fit S converged to a value near unity.

H atoms were placed at database-derived optimized distances from the carrier atom, which were reset after every refinement cycle, and refined with isotropic displacement parameters. To correctly assess the hydrogen bonds in the invariom model, bonding distances and angles were calculated using the module *XDGEOM* of *XD2016*. The result of the invariom refinement is shown in Fig. 1. The displacement ellipsoid plot for the IAM refinement is nearly identical.

2.3. Further computations

The electrostatic potential was directly derived from the invariom model using *XD2016* (Volkov *et al.*, 2016) and projected on the Hirshfeld surface using *MoleCoolQt* (Hübschle & Dittrich, 2011). The *Tonto* routines (Jayatilaka & Grimwood, 2003) implemented in *CrystalExplorer* (Turner *et al.*, 2017) were used to calculate Hirshfeld surfaces and fingerprint plots, as well as to compute scaled interaction energies *via* density-functional theory (DFT) with the hybrid functional B3LYP and Pople's polarized split-valence basis set 6-31G(d,p) (Mackenzie *et al.*, 2017).

3. Results and discussion

3.1. Invariom *versus* IAM refinement

The number of reflections used in both refinements deviate from each other because of algorithmic differences: *SHELXL*, the *de-facto* standard in conventional IAM refinements, adjusts against intensity data and includes all reflections in the final refinement steps (negative intensities below a modifiable threshold are set to the threshold value), whereas *XD2016* (Volkov *et al.*, 2016), the standard in charge-density studies, excludes the unobserved reflections. For the calculation of structure factors and R values, however, all reflections are included in both cases.

Under these preconditions, the invariom model outperformed the IAM in terms of R factors, especially $wR(F^2)$ for all reflections, and the r.m.s. of the difference electron-density $\Delta\rho$. Whereas the IAM exhibits local maxima at lone-pair positions, on delocalized π and also many σ bonds, the invarioms model bond and lone-pair electron density at the expense of core electron density. This is manifested in the deformation electron density $\Delta\rho_{\rm def} = \rho(\text{invariom}) - \rho(\text{IAM})$ (Fig. 2) clearly showing these features. As the results of the invariom refinement are superior to those of the IAM refinement, all the following considerations are based on the former.

3.2. Molecular geometry

All bond lengths within the molecule of (I) are in the expected range. The ethylene groups adopt – at least approximately – staggered conformations. Bonds to adjacent O atoms are oriented *gauche*, with the exception of the O1—C2—C3—O4 fragment, which shows an *anti* conformation. This results in an overall boat-like shape of the molecule, which is governed by two planes: one containing the chain segment C18–C29 (r.m.s. deviation = 0.0370 Å), roughly coinciding with the crystallographic plane (124), and one containing atoms O1–C13 and C29 (r.m.s. deviation = 0.1035 Å), roughly coinciding with $(\overline{1}25)$. The planes intersect at an angle of 76.377 (1)°. Atoms O14–O17 are part of neither plane (*cf.* Fig. S1 in the supporting information).

Interestingly, a comparison of the average displacement parameters for the shorter [$\overline{U}_{\rm eq}$(C/O)= 0.029 (4) Å^2 and $\overline{U}_{\rm iso}$(H) = 0.048 (6) Å^2] and the longer chain [$\overline{U}_{\rm eq}$(C/O) = 0.036 (4) Å^2 and $\overline{U}_{\rm iso}$(H) = 0.068 (6) Å^2] connecting the aromatic rings also hints at slightly less order in the latter. The maximum residual electron density is also found in its envir-

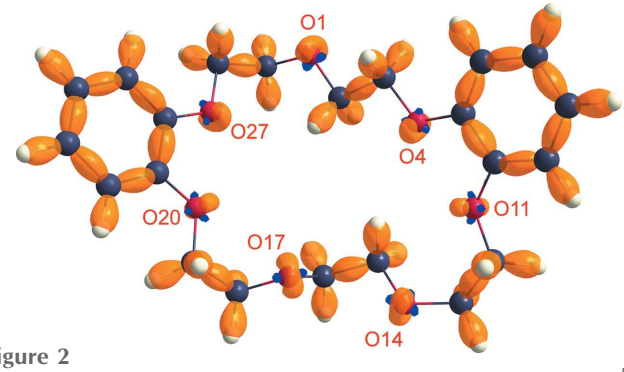

Figure 2
Isosurfaces of the deformation electron density $\Delta\rho_{\rm def} = \pm 0.3$ e Å^{-3} (positive is orange and negative is blue). The molecule is shown in a ball-and-stick representation with arbitrary radii (colour key: C atoms black, O atoms red and H atoms white).

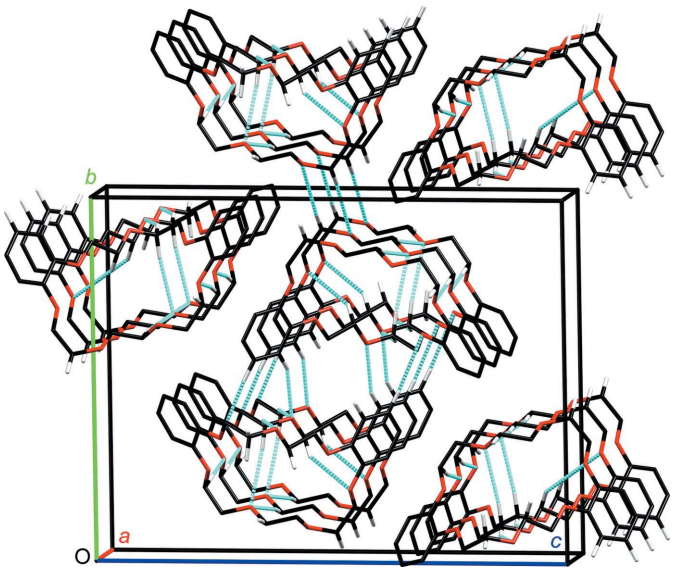

Figure 3
The packing diagram of (I) in the crystal, shown in a capped-stick representation with arbitrary radius (colour key: black C, red O and white H atoms, and blue dashed lines NCHBs). H atoms not involved in the hydrogen bonding and dangling hydrogen bonds have been omitted for clarity.

onment. The small increase when switching from the IAM to the invariom model (*cf.* Table 1) is due to the now adequate modelling of bond and lone-pair electron density; the effect of minor disorder becomes more pronounced. However, the high degree of order in the crystals remains exceptional for uncoordinated crown ethers.

3.3. Intermolecular interactions

3.3.1. Contacts and packing. Two kinds of intermolecular interactions govern the crystal packing, *i.e.* dispersive contacts and nonclassical hydrogen bonds (NCHBs) between C—H groups and O atoms. Among the dispersive contacts, various side-on interactions between aromatic rings and catechol CH_2 groups, as well as edge-on contacts between the out-of-plane part of the longer chain and the C21–C26 ring, are predominant.

To assess the hydrogen-bond network, we defined NCHBs using relatively strict criteria: C···O ≤ 4.5Å and C—H···O ≥ 150° (Desiraju & Steiner, 1999). Inspection of the twofold hydrogen-bonded H2*A* atom led to the rejection of the longer smaller-angle bond to atom O14 so that eight intermolecular NCHBs are considered to be present (see Table 2). Based on their C···O distance, seven of these may be grouped into one of two classes (3.80–4.10 and 4.25–4.45 Å). One bond is particularly short at 3.5631 (13) Å.

In the crystal, the boat-like molecules are stacked to build infinite chains along *a*, donating four and accepting one NCHB on the 'inner side' – and *vice versa* on the 'outer side' (Fig. 3). Three belong to the class of shorter NHCBs and two to the class of longer NHCBs. This correlates well with the results of computation: with a total energy of −88.8 kJ mol^{-1} per molecule (*cf.* Table S2 and Fig. S1 in the supporting information), the interactions in these chains are by far the strongest in the crystal. The shortest hydrogen bonds connect the chains to dimers, in which each molecule donates and accepts one NCHB of this type to/from the same neighbour related by a centre of inversion (Fig. 3, centre of the unit cell). In keeping with these hydrogen bonds being the shortest, one finds the second lowest electrostatic and total interaction energy (−29.1 kJ mol^{-1}) within the dimers. The remaining two longer NCHBs connect the chain dimers to form infinite rows (Fig. 3, upper cell boundary). Adjacent molecules interacting dispersively *via* aromatic rings exhibit total interaction energies of −22.6 to −21.0 kJ mol^{-1}, whereas other dispersive contacts are much higher in energy.

Table 2
Hydrogen-bond geometry (Å, °) for Invariom.

D—H···*A*	*D*—H	H···*A*	*D*···*A*	*D*—H···*A*
C2—H2*A*···O11^{i}	1.10	2.85	3.8410 (14)	151
C6—H6···O1^{ii}	1.08	2.57	3.5631 (13)	153
C7—H7···O27^{iii}	1.08	3.23	4.2104 (14)	151
C13—H13*B*···O14^{iv}	1.10	3.26	4.3405 (15)	170
C16—H16*A*···O17^{i}	1.10	3.21	4.2956 (16)	172
C19—H19*B*···O20^{v}	1.10	3.01	4.0769 (14)	164
C29—H29*A*···O17^{i}	1.10	2.85	3.9393 (15)	172
C29—H29*B*···O1^{i}	1.10	3.42	4.4459 (14)	156

Symmetry codes: (i) $x+1, y, z$; (ii) $-x+2, -y+1, -z+1$; (iii) $-x+1, -y+1, -z+1$; (iv) $-x, -y+2, -z+1$; (v) $x-1, y, z$.

The energy computations also confirmed that dispersive interactions are by far the strongest influence. Electrostatic interactions are only of minor importance, whereas polarization does not play any role at all.

3.3.2. Hirshfeld surface and fingerprint plot. Amongst the many possibilities to partition and assign crystallographic space with respect to molecular crystals, a variation of Hirshfeld's stockholder partitioning (Hirshfeld, 1977) has become exceedingly popular. In this scheme, the surface assigned to a molecule encloses that volume in which the promolecule contribution from this molecule – constructed from nuclear positions and spherically averaged electron density – exceeds that of all neighbouring molecules (Spackman & Byrom, 1997).

The information conveyed by shape representations of the Hirshfeld surface can be enhanced by colour-coding properties onto it. Fig. 4 (top) shows a projection of the normalized contact distance $d_{\rm norm}$. Areas in which the distance between adjacent molecules is smaller and greater than the sum of their van der Waals radii are marked in red and blue, respectively. A first introspection already makes clear that most contacts are longer than (blue) or approximately equal to (white, especially along the molecular perimeter) the values expected from the van der Waals radii. Two exceptions are, however, distinguishable (red), *viz.* a side-on C—H···π contact between atom H28*B* and the C21–C26 ring (atom–plane distance = 2.544 Å) and a side-on C—H···H—C contact between atoms H23 and H13*A* (distance = 2.314 Å).

The two-dimensional fingerprint plot of a Hirshfeld surface summarizes the intermolecular interactions in a crystal. For

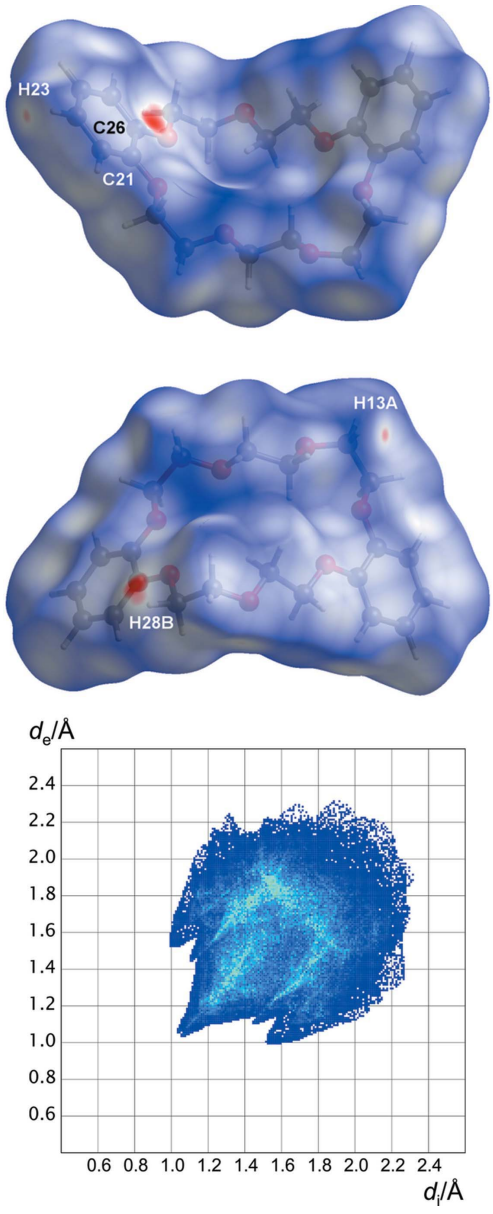

Figure 4
(Top) Hirshfeld surface with projection of the normalized contact distance d_{norm} in two orientations (colour key: blue is positive, white is zero and red is negative). The molecule is shown in a ball-and-stick representation with arbitrary radii (colour key: C atoms black, O atoms red and H atoms white). (Bottom) A fingerprint plot of the Hirshfeld surface with external and internal distances, *i.e.* d_e and d_i. The colours indicate the surface-area fraction, with a rainbow scheme ranging from blue (small) to red (large).

every point of the Hirshfeld surface, the distance d_i from the nearest nucleus inside *versus* the distance d_e from the nearest nucleus outside is plotted. Colour is used to encode the number of times each pair of distances occurs, equalling the respective surface-area fraction (see Fig. 4, bottom). The absence of colours in the range from yellow to red and the comparatively large spread ($1.0 \leq d \leq 2.3$ Å) show that the distance pairs are quite evenly distributed. This can be attributed to the anisotropic molecular shape giving rise to a variety of different contacts (Spackman & McKinnon, 2002). Nevertheless, some features are discernible. The pale-green band roughly along the line defined by $d_e = d_i$ is due to the numerous dispersive head-to-head H···H interactions, while the pale-green bands below and above are caused by C—H···O interactions, *i.e.* the NCHBs. The blue wing-like structures, which are located even further out, result from C—H···π contacts. The brightest feature at $d_e \simeq 1.9$ Å, $d_i \simeq 1.5$Å derives from an overlap of predominant H···H (between aliphatic, as well as between aliphatic and aromatic parts) and some C—H···O interactions.

3.3.3. Electrostatic potential. Although electrostatic interactions are of minor importance (*cf.* §3.3.1), a short survey is in order for the sake of completeness. The electrostatic potential $V(\boldsymbol{r})$ at the point $\boldsymbol{r}$ is available from the final structural parameters and the predicted multipoles of an invariom refinement. For (I), it is illustrated in Fig. 5.

From the picture, it is evident that regions of high potential are located at the H atoms on the molecular perimeter, especially on the aromatic rings. Regions of low potential are located near the central fold dominated by O atoms, especially O14 and O17, and those stemming from catechol. It is safe to assume that what are overall relatively weak electrostatic interactions manifest primarily in NCHBs, as these are the predominant C—H···O contacts. The findings are thus in tune with atom O17 accepting two hydrogen bonds, and O14 accepting one NCHB and having a relatively strong interaction with atom H2*A* (*cf.* §3.3.1). The electrostatic interaction energies (*cf.* Table S2 and Fig. S1 in the supporting information) nicely reflect the number of NCHBs between neighbouring molecules, as well as the adjacenct nature of regions of opposite potential: they are the lowest (unscaled −29.7 kJ mol^{-1}) for the stacks along *a* and, remarkably second in place, for the dimers bound *via* hydrogen bonds of the shortest type (unscaled −11.0 kJ mol^{-1}).

4. Conclusion

Well-ordered solvent-free crystals of dibenzo-21-crown-7 can be grown from a solution in toluene *via* slow evaporation using a small temperature gradient. The tendency of crown ethers to form cocrystals with solvent molecules can be reduced using

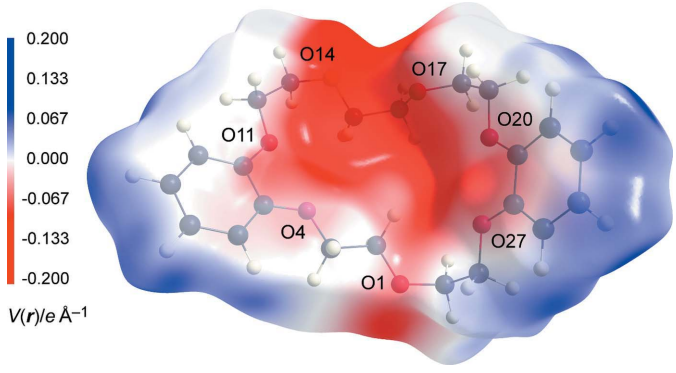

Figure 5
Electrostatic potential projected on the Hirshfeld surface. The molecule is shown in a ball-and-stick representation with arbitrary radii (colour key: C atoms black, O atoms red and H atoms white).

apolar solvents. This is crucial in order not to disrupt dispersive contacts between crown-ether molecules in favour of stronger electrostatic interactions with solvent molecules.

The predominant intermolecular interactions in the crystal are of a dispersive nature and are manifested in various C—H···H—C and C—H···π contacts. In addition, nonclassical C—H···O hydrogen bonds are abundant, based on dispersive, as well as much weaker electrostatic interaction. The boat-like conformation of the molecules enables efficient stacking along the *a* axis so that multiple weak dispersive contacts and hydrogen bonds contribute to a relatively strong total attraction between pairs of molecules in an infinite stack. Further, this motif seems to impose order even on a notoriously 'difficult group', such as the –O[(–CH_2)$_2$–O]$_3$– chain.

Acknowledgements

We thank Professor Andreas Grohmann (Technische Universität Berlin) for fruitful discussion, Dr Christian Hübschle (Universität Bayreuth) for help getting started with the *MoleCoolQt* and *XD2016* software, and Ms Paula Nixdorf (Technische Universität Berlin) for collecting the diffraction data.

References

Blasius, E. & Nilles, K.-H. (1984). *Radiochim. Acta*, **35**, 173–182.
Burns, J. H., Bryan, J. C., Davis, M. C. & Sachleben, R. A. (1996). *J. Inclusion Phenom. Mol. Recognit. Chem.* **26**, 197–207.
Chemical Abstracts Service (2017). RN 14098-41-0. Columbus, Ohio, USA (accessed *via* SciFinder on July 7, 2017).
Desiraju, G. & Steiner, T. (1999). In *The Weak Hydrogen Bond in Structural Chemistry and Biology*. Oxford University Press.
Dittrich, B., Hübschle, C. B., Pröpper, K., Dietrich, F., Stolper, T. & Holstein, J. J. (2013). *Acta Cryst.* B**69**, 91–104.
Dittrich, B., Koritsánszky, T. & Luger, P. (2004). *Angew. Chem. Int. Ed.* **43**, 2718–2721.
Dolomanov, O. V., Bourhis, L. J., Gildea, R. J., Howard, J. A. K. & Puschmann, H. (2009). *J. Appl. Cryst.* **42**, 339–341.
Farrugia, L. J. (2012). *J. Appl. Cryst.* **45**, 849–854.
Hansen, N. K. & Coppens, P. (1978). *Acta Cryst.* A**34**, 909–921.
Hirshfeld, F. L. (1977). *Theor. Chim. Acta*, **44**, 129–138.
Hübschle, C. B. & Dittrich, B. (2011). *J. Appl. Cryst.* **44**, 238–240.
Jayatilaka, D. & Grimwood, D. J. (2003). *Computational Science – ICCS 2003*, edited by P. M. A. Sloot, D. Abramson, A. V. Bogdanov, Y. E. Gorbachev, J. J. Dongarra & A. Y. Zomaya, pp. 142–151. Berlin: Springer.
Mackenzie, C. F., Spackman, P. R., Jayatilaka, D. & Spackman, M. A. (2017). IUCrJ, **4**. https://doi.org/10.1107/S205225251700848X.
Macrae, C. F., Bruno, I. J., Chisholm, J. A., Edgington, P. R., McCabe, P., Pidcock, E., Rodriguez-Monge, L., Taylor, R., van de Streek, J. & Wood, P. A. (2008). *J. Appl. Cryst.* **41**, 466–470.
Mäkelä, T., Kiesilä, A., Kalenius, E. & Rissanen, K. (2016). *Chem. Eur. J.* **22**, 14264–14272.
Owen, J. D. & Nowell, I. W. (1978). *Acta Cryst.* B**34**, 2354–2356.
Pedersen, C. J. (1967). *J. Am. Chem. Soc.* **89**, 7017–7036.
Rigaku Oxford Diffraction (2015). *CrysAlis PRO*. Rigaku Corporation, Yarnton, Oxfordshire, England.
Sachleben, R. A., Bryan, J. C., Lavis, J. M., Starks, C. M. & Burns, J. H. (1997). *Tetrahedron*, **53**, 13567–13582.
Sanjuan-Szklarz, W. F., Hoser, A. A., Gutmann, M., Madsen, A. Ø. & Wozniak, K. (2016). *IUCrJ*, **3**, 61–70.
Sheldrick, G. M. (2015*a*). *Acta Cryst.* A**71**, 3–8.
Sheldrick, G. M. (2015*b*). *Acta Cryst.* C**71**, 3–8.
Spackman, M. A. & Byrom, P. G. (1997). *Chem. Phys. Lett.* **267**, 215–220.
Spackman, M. A. & McKinnon, J. J. (2002). *CrystEngComm*, **4**, 378–392.
Turner, M. J., McKinnon, J. J., Wolff, S. K., Grimwood, D. J., Spackman, P. R., Jayatilaka, D. & Spackman, M. A. (2017). *CrystalExplorer*. University of Western Australia, Australia.
Volkov, A., Macchi, P., Farrugia, L. J., Gatti, C., Mallinson, P., Richter, T. & Koritsánszky, T. (2016). *XD2016*. University of New York at Buffalo, New York, USA.

supporting information

Acta Cryst. (2017). C**73**, 654-659 [https://doi.org/10.1107/S2053229617011160]

Invariom-model refinement and Hirshfeld surface analysis of well-ordered solvent-free dibenzo-21-crown-7

Dennis Wiedemann and Julia Kohl

Computing details

For both structures, data collection: *CrysAlis PRO* (Rigaku Oxford Diffraction, 2015); cell refinement: *CrysAlis PRO* (Rigaku Oxford Diffraction, 2015); data reduction: *CrysAlis PRO* (Rigaku Oxford Diffraction, 2015); program(s) used to solve structure: SHELXT (Sheldrick, 2015a). Program(s) used to refine structure: XD2016 (Volkov *et al.*, 2016) for Invariom; *SHELXL2016* (Sheldrick, 2015b) for IAM. For both structures, molecular graphics: *ORTEP-3 for Windows* (Farrugia, 2012) and *Mercury* (Macrae *et al.*, 2008). Software used to prepare material for publication: WinXD (Volkov *et al.*, 2016) for Invariom; OLEX2 (Dolomanov *et al.*, 2009) for IAM.

Dibenzo[*b*,*k*][1,4,7,10,13,16,19]heptaoxacyclohenicosa-2,11-diene (Invariom)

Crystal data

$C_{22}H_{28}O_7$
M_r = 404.44
Monoclinic, $P2_1/c$
a = 4.9801 (1) Å
b = 17.4771 (2) Å
c = 23.1000 (2) Å
β = 94.124 (1)°
V = 2005.37 (5) Å^3
Z = 4
$F(000)$ = 864
D_x = 1.34 Mg m^{-3}
Melting point: 388 K
Cu $K\alpha$ radiation, λ = 1.54184 Å
Cell parameters from 7438 reflections
θ = 2.5–73.5°
μ = 0.82 mm^{-1}
T = 150 K
Shard, colourless
0.74 × 0.14 × 0.08 mm

Data collection

Agilent SuperNova (single source) diffractometer
Radiation source: micro-focus sealed tube, Agilent Nova
Mirror monochromator
Detector resolution: 10.5435 pixels mm^{-1}
ω scans
Absorption correction: gaussian (CrysAlis PRO; Rigaku Oxford Diffraction, 2015)
T_{min} = 0.598, T_{max} = 1.000
13236 measured reflections
3925 independent reflections
3559 reflections with $I > 2\sigma(I)$
R_{int} = 0.018
θ_{max} = 73.7°, θ_{min} = 3.2°
h = −5→6
k = −21→21
l = −27→28

Refinement

Refinement on F^2
Least-squares matrix: full
$R[F^2 > 2\sigma(F^2)]$ = 0.030
$wR(F^2)$ = 0.084
S = 0.98
3664 reflections
290 parameters
0 restraints

Primary atom site location: dual
Hydrogen site location: difference Fourier map
Only H-atom displacement parameters refined

$w = 1/[\sigma^2(F_o^2) + (0.0497P)^2 + 0.1P]$
where $P = (F_o^2 + 2F_c^2)/3$
$(\Delta/\sigma)_{max} < 0.001$
$\Delta\rho_{max} = 0.41$ e Å^{-3}
$\Delta\rho_{min} = -0.24$ e Å^{-3}

Special details

Refinement. After conventional IAM refinement, invarioms were assigned and set up using MoleCoolQt Revision 558 (Hübschle & Dittrich, 2011).
All hydrogen atoms were reset to neutron-diffraction–derived distances to their carrier atoms after every refinement cycle (d = 1.0962 Å for methylene groups, d = 1.0823 Å for aromatics).

Fractional atomic coordinates and isotropic or equivalent isotropic displacement parameters (Å²)

	x	*y*	*z*	U_{iso}*/U_{eq}
C2	1.0446 (2)	0.65479 (6)	0.55315 (5)	0.027
H2A	1.15515	0.70408	0.537643	0.056 (5)*
H2B	0.921845	0.673982	0.587914	0.051 (4)*
C3	0.8678 (2)	0.61989 (6)	0.50382 (5)	0.026
H3A	0.99184	0.597868	0.470203	0.040 (4)*
H3B	0.749237	0.572587	0.519914	0.042 (4)*
C5	0.5121 (2)	0.66085 (6)	0.43710 (4)	0.024
C6	0.4908 (2)	0.58977 (6)	0.41032 (5)	0.027
H6	0.628561	0.544207	0.423852	0.043 (4)*
C7	0.2899 (2)	0.57697 (7)	0.36562 (5)	0.03
H7	0.275295	0.52187	0.344238	0.053 (4)*
C8	0.1099 (2)	0.63436 (7)	0.34872 (5)	0.031
H8	−0.046729	0.623725	0.314726	0.057 (5)*
C9	0.1296 (2)	0.70607 (6)	0.37537 (5)	0.028
H9	−0.011815	0.750858	0.362114	0.051 (4)*
C10	0.3311 (2)	0.71984 (6)	0.41890 (4)	0.024
C12	0.1553 (2)	0.84115 (7)	0.44408 (5)	0.033
H12A	−0.023216	0.814777	0.460837	0.061 (5)*
H12B	0.104154	0.859291	0.399212	0.060 (5)*
C13	0.2414 (3)	0.90954 (7)	0.48096 (5)	0.037
H13A	0.424768	0.933229	0.46439	0.064 (5)*
H13B	0.08429	0.953382	0.475337	0.064 (5)*
C15	0.5459 (3)	0.85914 (8)	0.55510 (6)	0.041
H15A	0.69461	0.880486	0.526282	0.075 (6)*
H15B	0.528137	0.797078	0.549115	0.081 (6)*
C16	0.6417 (3)	0.87561 (8)	0.61654 (6)	0.04
H16A	0.854031	0.859333	0.623821	0.092 (7)*
H16B	0.624433	0.937083	0.624937	0.075 (6)*
C18	0.5696 (3)	0.84899 (7)	0.71319 (6)	0.039
H18A	0.450759	0.896087	0.729498	0.069 (6)*
H18B	0.781893	0.866109	0.716492	0.066 (5)*
C19	0.5354 (2)	0.77896 (6)	0.74960 (5)	0.032
H19A	0.561502	0.793497	0.795824	0.054 (4)*
H19B	0.33372	0.754776	0.740426	0.057 (5)*

C21	0.7616 (2)	0.66022 (6)	0.76552 (5)	0.026
C22	0.6192 (2)	0.64273 (6)	0.81330 (5)	0.03
H22	0.476384	0.683409	0.828543	0.054 (4)*
C23	0.6593 (2)	0.57272 (7)	0.84169 (5)	0.034
H23	0.547514	0.559374	0.87888	0.059 (5)*
C24	0.8413 (2)	0.52029 (7)	0.82286 (5)	0.034
H24	0.871798	0.466227	0.845215	0.050 (4)*
C25	0.9859 (2)	0.53724 (6)	0.77468 (5)	0.03
H25	1.129405	0.496312	0.760065	0.055 (4)*
C26	0.9465 (2)	0.60623 (6)	0.74558 (5)	0.026
C28	1.2705 (2)	0.57778 (6)	0.67776 (5)	0.026
H28A	1.182808	0.521846	0.666116	0.045 (4)*
H28B	1.432227	0.569403	0.711938	0.043 (4)*
C29	1.3829 (2)	0.61374 (7)	0.62490 (5)	0.029
H29A	1.391005	0.675946	0.630839	0.051 (4)*
H29B	1.589078	0.59329	0.621268	0.054 (5)*
O1	1.22374 (18)	0.59660 (5)	0.57328 (4)	0.037
O4	0.69566 (15)	0.67931 (4)	0.48120 (3)	0.028
O11	0.37270 (15)	0.78813 (4)	0.44647 (3)	0.03
O14	0.29216 (18)	0.89459 (5)	0.54075 (4)	0.04
O17	0.48593 (19)	0.83406 (5)	0.65485 (4)	0.041
O20	0.73637 (16)	0.72575 (4)	0.73461 (4)	0.033
O27	1.06943 (15)	0.62756 (5)	0.69748 (3)	0.031

Atomic displacement parameters (Å²)

	U^{11}	U^{22}	U^{33}	U^{12}	U^{13}	U^{23}
C2	0.0249 (5)	0.0283 (5)	0.0278 (5)	0.0033 (4)	−0.0007 (4)	−0.0021 (4)
C3	0.0234 (5)	0.0272 (5)	0.0270 (5)	0.0028 (4)	−0.0005 (4)	−0.0013 (4)
C5	0.0203 (5)	0.0241 (5)	0.0262 (5)	0.0025 (4)	0.0008 (4)	−0.0020 (4)
C6	0.0228 (5)	0.0246 (5)	0.0330 (6)	0.0032 (4)	−0.0010 (4)	−0.0055 (4)
C7	0.0264 (6)	0.0293 (6)	0.0342 (6)	0.0012 (4)	−0.0033 (4)	−0.0068 (4)
C8	0.0272 (6)	0.0326 (6)	0.0313 (6)	0.0014 (4)	−0.0051 (4)	−0.0021 (5)
C9	0.0264 (5)	0.0289 (6)	0.0294 (5)	0.0031 (4)	−0.0027 (4)	0.0018 (4)
C10	0.0237 (5)	0.0234 (5)	0.0259 (5)	0.0038 (4)	0.0013 (4)	0.0006 (4)
C12	0.0358 (6)	0.0281 (6)	0.0340 (6)	0.0106 (5)	0.0025 (5)	−0.0001 (5)
C13	0.0508 (8)	0.0278 (6)	0.0342 (6)	0.0113 (5)	0.0060 (5)	−0.0023 (5)
C15	0.0394 (7)	0.0482 (8)	0.0350 (7)	0.0064 (6)	0.0050 (5)	−0.0052 (6)
C16	0.0397 (7)	0.0396 (7)	0.0394 (7)	−0.0005 (5)	0.0035 (5)	−0.0083 (5)
C18	0.0516 (8)	0.0280 (6)	0.0361 (6)	0.0036 (5)	−0.0010 (5)	−0.0021 (5)
C19	0.0353 (6)	0.0281 (6)	0.0319 (6)	0.0056 (5)	0.0031 (5)	−0.0034 (4)
C21	0.0246 (5)	0.0245 (5)	0.0282 (5)	−0.0006 (4)	0.0025 (4)	−0.0054 (4)
C22	0.0311 (6)	0.0280 (5)	0.0315 (6)	−0.0019 (4)	0.0058 (4)	−0.0041 (4)
C23	0.0366 (6)	0.0314 (6)	0.0339 (6)	−0.0043 (5)	0.0063 (5)	−0.0006 (5)
C24	0.0345 (6)	0.0286 (6)	0.0384 (6)	−0.0022 (5)	0.0023 (5)	0.0029 (5)
C25	0.0272 (6)	0.0269 (6)	0.0362 (6)	0.0006 (4)	0.0005 (4)	−0.0007 (5)
C26	0.0216 (5)	0.0255 (5)	0.0300 (5)	0.0006 (4)	0.0001 (4)	−0.0042 (4)
C28	0.0200 (5)	0.0287 (5)	0.0303 (5)	0.0027 (4)	−0.0011 (4)	−0.0049 (4)

C29	0.0244 (5)	0.0330 (6)	0.0293 (5)	0.0034 (4)	−0.0004 (4)	−0.0023 (4)
O1	0.0432 (5)	0.0342 (4)	0.0319 (4)	0.0131 (4)	−0.0102 (4)	−0.0083 (3)
O4	0.0251 (4)	0.0261 (4)	0.0311 (4)	0.0045 (3)	−0.0034 (3)	−0.0041 (3)
O11	0.0291 (4)	0.0252 (4)	0.0343 (4)	0.0055 (3)	−0.0003 (3)	−0.0034 (3)
O14	0.0411 (5)	0.0465 (5)	0.0322 (4)	0.0101 (4)	0.0081 (4)	−0.0028 (4)
O17	0.0489 (5)	0.0393 (5)	0.0349 (5)	−0.0029 (4)	−0.0011 (4)	0.0011 (4)
O20	0.0358 (4)	0.0283 (4)	0.0353 (4)	0.0053 (3)	0.0093 (3)	−0.0001 (3)
O27	0.0284 (4)	0.0310 (4)	0.0332 (4)	0.0059 (3)	0.0055 (3)	−0.0004 (3)

Geometric parameters (Å, º)

C2—H2A	1.0962	C16—H16A	1.0962
C2—H2B	1.0962	C16—H16B	1.0963
C2—C3	1.5171 (15)	C16—O17	1.4181 (16)
C2—O1	1.4095 (13)	C18—H18A	1.0962
C3—H3A	1.0963	C18—H18B	1.0962
C3—H3B	1.0963	C18—C19	1.5015 (17)
C3—O4	1.4221 (12)	C18—O17	1.4060 (15)
C5—C6	1.3885 (15)	C19—H19A	1.0962
C5—C10	1.4135 (14)	C19—H19B	1.0962
C5—O4	1.3577 (12)	C19—O20	1.4270 (13)
C6—H6	1.0822	C21—C22	1.3882 (15)
C6—C7	1.4033 (15)	C21—C26	1.4184 (14)
C7—H7	1.0822	C21—O20	1.3507 (13)
C7—C8	1.3827 (16)	C22—H22	1.0822
C8—H8	1.0823	C22—C23	1.3957 (17)
C8—C9	1.3966 (16)	C23—H23	1.0823
C9—H9	1.0822	C23—C24	1.3810 (17)
C9—C10	1.3896 (15)	C24—H24	1.0823
C10—O11	1.3618 (13)	C24—C25	1.3999 (17)
C12—H12A	1.0963	C25—H25	1.0823
C12—H12B	1.0962	C25—C26	1.3875 (16)
C12—C13	1.5120 (17)	C26—O27	1.3589 (13)
C12—O11	1.4232 (13)	C28—H28A	1.0963
C13—H13A	1.0962	C28—H28B	1.0962
C13—H13B	1.0962	C28—C29	1.5157 (16)
C13—O14	1.4105 (15)	C28—O27	1.4258 (12)
C15—H15A	1.0963	C29—H29A	1.0963
C15—H15B	1.0962	C29—H29B	1.0962
C15—C16	1.4924 (18)	C29—O1	1.4155 (13)
C15—O14	1.4248 (16)		
H2A—C2—H2B	108.58	H16A—C16—O17	109.65
H2A—C2—C3	110.40	H16B—C16—O17	109.76
H2A—C2—O1	110.73	H18A—C18—H18B	108.23
H2B—C2—C3	110.43	H18A—C18—C19	109.50
H2B—C2—O1	110.62	H18A—C18—O17	109.79
C3—C2—O1	106.08 (8)	H18B—C18—C19	109.34

C2—C3—H3A	110.31	H18B—C18—O17	109.58
C2—C3—H3B	110.26	C19—C18—O17	110.36 (10)
C2—C3—O4	106.52 (8)	C18—C19—H19A	110.27
H3A—C3—H3B	108.67	C18—C19—H19B	110.20
H3A—C3—O4	110.58	C18—C19—O20	106.59 (9)
H3B—C3—O4	110.49	H19A—C19—H19B	108.69
C6—C5—C10	119.56 (10)	H19A—C19—O20	110.56
C6—C5—O4	124.93 (9)	H19B—C19—O20	110.53
C10—C5—O4	115.50 (9)	C22—C21—C26	119.50 (10)
C5—C6—H6	120.20	C22—C21—O20	125.01 (10)
C5—C6—C7	119.87 (10)	C26—C21—O20	115.49 (9)
H6—C6—C7	119.93	C21—C22—H22	119.95
C6—C7—H7	119.90	C21—C22—C23	120.17 (10)
C6—C7—C8	120.38 (10)	H22—C22—C23	119.88
H7—C7—C8	119.72	C22—C23—H23	119.83
C7—C8—H8	119.93	C22—C23—C24	120.58 (11)
C7—C8—C9	120.20 (10)	H23—C23—C24	119.59
H8—C8—C9	119.87	C23—C24—H24	120.11
C8—C9—H9	120.05	C23—C24—C25	119.78 (11)
C8—C9—C10	119.90 (10)	H24—C24—C25	120.10
H9—C9—C10	120.05	C24—C25—H25	119.81
C5—C10—C9	120.06 (10)	C24—C25—C26	120.41 (11)
C5—C10—O11	115.32 (9)	H25—C25—C26	119.78
C9—C10—O11	124.61 (9)	C21—C26—C25	119.56 (10)
H12A—C12—H12B	108.44	C21—C26—O27	115.11 (9)
H12A—C12—C13	109.75	C25—C26—O27	125.33 (10)
H12A—C12—O11	110.28	H28A—C28—H28B	108.47
H12B—C12—C13	109.95	H28A—C28—C29	109.61
H12B—C12—O11	110.44	H28A—C28—O27	110.23
C13—C12—O11	107.97 (10)	H28B—C28—C29	109.93
C12—C13—H13A	108.15	H28B—C28—O27	110.36
C12—C13—H13B	108.33	C29—C28—O27	108.23 (9)
C12—C13—O14	115.39 (10)	C28—C29—H29A	108.84
H13A—C13—H13B	107.46	C28—C29—H29B	109.19
H13A—C13—O14	108.47	C28—C29—O1	111.98 (9)
H13B—C13—O14	108.76	H29A—C29—H29B	107.85
H15A—C15—H15B	108.18	H29A—C29—O1	109.19
H15A—C15—C16	109.15	H29B—C29—O1	109.72
H15A—C15—O14	109.71	C2—O1—C29	115.34 (8)
H15B—C15—C16	109.15	C3—O4—C5	117.24 (8)
H15B—C15—O14	109.80	C10—O11—C12	117.56 (8)
C16—C15—O14	110.79 (10)	C13—O14—C15	113.69 (9)
C15—C16—H16A	109.56	C16—O17—C18	111.43 (10)
C15—C16—H16B	109.48	C19—O20—C21	117.68 (9)
C15—C16—O17	110.05 (11)	C26—O27—C28	117.51 (9)
H16A—C16—H16B	108.31		
H2A—C2—C3—H3A	63.05	C16—C15—O14—C13	154.91 (14)

H2A—C2—C3—H3B	−176.92	O14—C15—C16—H16A	−167.24
H2A—C2—C3—O4	−57.00	O14—C15—C16—H16B	−48.60
H2A—C2—O1—C29	68.75	O14—C15—C16—O17	72.12 (12)
H2B—C2—C3—H3A	−176.87	C15—C16—O17—C18	−179.38 (14)
H2B—C2—C3—H3B	−56.83	H16A—C16—O17—C18	60.04 (11)
H2B—C2—C3—O4	63.08	H16B—C16—O17—C18	−58.83
H2B—C2—O1—C29	−51.67	H18A—C18—C19—H19A	−47.69
O1—C2—C3—H3A	−56.97	H18A—C18—C19—H19B	72.30
O1—C2—C3—H3B	63.07	H18A—C18—C19—O20	−167.74
C3—C2—O1—C29	−171.45 (12)	H18A—C18—O17—C16	92.57
O1—C2—C3—O4	−177.02 (11)	H18B—C18—C19—H19A	70.74
C2—C3—O4—C5	−178.27 (12)	H18B—C18—C19—H19B	−169.27
H3A—C3—O4—C5	61.85	H18B—C18—C19—O20	−49.31
H3B—C3—O4—C5	−58.50	H18B—C18—O17—C16	−26.18
C10—C5—C6—H6	179.91 (16)	C19—C18—O17—C16	−146.64 (14)
C10—C5—C6—C7	−0.19 (10)	O17—C18—C19—H19A	−168.66
C6—C5—C10—C9	1.44 (10)	O17—C18—C19—H19B	−48.67
C6—C5—C10—O11	−178.08 (14)	O17—C18—C19—O20	71.29 (11)
C6—C5—O4—C3	−4.01 (10)	C18—C19—O20—C21	174.35 (13)
O4—C5—C6—H6	−0.88	H19A—C19—O20—C21	54.49
O4—C5—C6—C7	179.03 (16)	H19B—C19—O20—C21	−65.90
C10—C5—O4—C3	175.23 (13)	C26—C21—C22—H22	−179.44
O4—C5—C10—C9	−177.85 (14)	C26—C21—C22—C23	0.42 (10)
O4—C5—C10—O11	2.63 (8)	C22—C21—C26—C25	−1.08 (10)
C5—C6—C7—H7	178.98	C22—C21—C26—O27	177.96 (15)
C5—C6—C7—C8	−1.08 (10)	C22—C21—O20—C19	−4.50 (10)
H6—C6—C7—H7	−1.12	O20—C21—C22—H22	−0.55
H6—C6—C7—C8	178.82	O20—C21—C22—C23	179.31 (17)
C6—C7—C8—H8	−178.94	C26—C21—O20—C19	174.42 (14)
C6—C7—C8—C9	1.11 (11)	O20—C21—C26—C25	179.93 (15)
H7—C7—C8—H8	1.00	O20—C21—C26—O27	−1.03 (9)
H7—C7—C8—C9	−178.95	C21—C22—C23—H23	−179.90 (18)
C7—C8—C9—H9	−179.89 (17)	C21—C22—C23—C24	0.29 (11)
C7—C8—C9—C10	0.15 (11)	H22—C22—C23—H23	−0.04 (10)
H8—C8—C9—H9	0.15 (10)	H22—C22—C23—C24	−179.85 (18)
H8—C8—C9—C10	−179.80 (17)	C22—C23—C24—H24	179.75 (18)
C8—C9—C10—C5	−1.42 (10)	C22—C23—C24—C25	−0.35 (11)
C8—C9—C10—O11	178.05 (17)	H23—C23—C24—H24	−0.05 (10)
H9—C9—C10—C5	178.62	H23—C23—C24—C25	179.84 (18)
H9—C9—C10—O11	−1.91	C23—C24—C25—H25	179.62 (18)
C5—C10—O11—C12	−160.57 (13)	C23—C24—C25—C26	−0.32 (11)
C9—C10—O11—C12	19.94 (10)	H24—C24—C25—H25	−0.48 (10)
H12A—C12—C13—H13A	177.62	H24—C24—C25—C26	179.58 (18)
H12A—C12—C13—H13B	−66.19	C24—C25—C26—C21	1.03 (10)
H12A—C12—C13—O14	55.97	C24—C25—C26—O27	−177.91 (17)
H12A—C12—O11—C10	56.09	H25—C25—C26—C21	−178.92
H12B—C12—C13—H13A	−63.17	H25—C25—C26—O27	2.15
H12B—C12—C13—H13B	53.01	C21—C26—O27—C28	175.91 (13)

H12B—C12—C13—O14	175.18	C25—C26—O27—C28	−5.11 (10)
H12B—C12—O11—C10	−63.75	H28A—C28—C29—H29A	156.43
C13—C12—O11—C10	176.00 (13)	H28A—C28—C29—H29B	−86.08
O11—C12—C13—H13A	57.38	H28A—C28—C29—O1	35.63
O11—C12—C13—H13B	173.57	H28A—C28—O27—C26	61.37
O11—C12—C13—O14	−64.27 (11)	H28B—C28—C29—H29A	−84.43
C12—C13—O14—C15	77.86 (12)	H28B—C28—C29—H29B	33.06
H13A—C13—O14—C15	−43.62	H28B—C28—C29—O1	154.77
H13B—C13—O14—C15	−160.21	H28B—C28—O27—C26	−58.42
H15A—C15—C16—H16A	−46.32	C29—C28—O27—C26	−178.76 (12)
H15A—C15—C16—H16B	72.32	O27—C28—C29—H29A	36.17
H15A—C15—C16—O17	−166.96	O27—C28—C29—H29B	153.66
H15A—C15—O14—C13	34.32	O27—C28—C29—O1	−84.63 (10)
H15B—C15—C16—H16A	71.73	C28—C29—O1—C2	99.84 (11)
H15B—C15—C16—H16B	−169.63	H29A—C29—O1—C2	−20.76
H15B—C15—C16—O17	−48.91	H29B—C29—O1—C2	−138.75
H15B—C15—O14—C13	−84.44		

Hydrogen-bond geometry (Å, º)

D—H···*A*	*D*—H	H···*A*	*D*···*A*	*D*—H···*A*
C2—H2*A*···O11^{i}	1.10	2.85	3.8410 (14)	151
C6—H6···O1^{ii}	1.08	2.57	3.5631 (13)	153
C7—H7···O27^{iii}	1.08	3.23	4.2104 (14)	151
C13—H13*B*···O14^{iv}	1.10	3.26	4.3405 (15)	170
C16—H16*A*···O17^{i}	1.10	3.21	4.2956 (16)	172
C19—H19*B*···O20^{v}	1.10	3.01	4.0769 (14)	164
C29—H29*A*···O17^{i}	1.10	2.85	3.9393 (15)	172
C29—H29*B*···O1^{i}	1.10	3.42	4.4459 (14)	156

Symmetry codes: (i) *x*+1, *y*, *z*; (ii) −*x*+2, −*y*+1, −*z*+1; (iii) −*x*+1, −*y*+1, −*z*+1; (iv) −*x*, −*y*+2, −*z*+1; (v) *x*−1, *y*, *z*.

Dibenzo[*b*,*k*][1,4,7,10,13,16,19]heptaoxacyclohenicosa-2,11-diene (IAM)

Crystal data

$C_{22}H_{28}O_7$
M_r = 404.44
Monoclinic, $P2_1/c$
a = 4.9801 (1) Å
b = 17.4771 (2) Å
c = 23.1000 (2) Å
β = 94.124 (1)°
V = 2005.37 (5) Å^3
Z = 4
F(000) = 864

D_x = 1.340 Mg m^{-3}
Melting point: 388 K
Cu $K\alpha$ radiation, λ = 1.54184 Å
Cell parameters from 7438 reflections
θ = 2.5–73.5°
μ = 0.82 mm^{-1}
T = 150 K
Shard, colourless
0.74 × 0.14 × 0.08 mm

Data collection

Agilent SuperNova (Single Source) diffractometer
Radiation source: micro-focus sealed tube, Agilent Nova

Mirror monochromator
Detector resolution: 10.5435 pixels mm^{-1}
ω scans

Absorption correction: gaussian (CrysAlis PRO; Rigaku Oxford Diffraction, 2015)
T_{min} = 0.598, T_{max} = 1.000
13236 measured reflections
3925 independent reflections

3559 reflections with $I > 2\sigma(I)$
R_{int} = 0.018
θ_{max} = 73.7°, θ_{min} = 3.2°
h = −5→6
k = −21→21
l = −27→28

Refinement

Refinement on F^2
Least-squares matrix: full
$R[F^2 > 2\sigma(F^2)]$ = 0.038
$wR(F^2)$ = 0.103
S = 1.05
3925 reflections
262 parameters
0 restraints

Primary atom site location: dual
Hydrogen site location: difference Fourier map
H-atom parameters constrained
$w = 1/[\sigma^2(F_o^2) + (0.0497P)^2 + 0.7337P]$ where $P = (F_o^2 + 2F_c^2)/3$
$(\Delta/\sigma)_{max} < 0.001$
$\Delta\rho_{max}$ = 0.39 e Å^{-3}
$\Delta\rho_{min}$ = −0.28 e Å^{-3}

Special details

Geometry. All esds (except the esd in the dihedral angle between two l.s. planes) are estimated using the full covariance matrix. The cell esds are taken into account individually in the estimation of esds in distances, angles and torsion angles; correlations between esds in cell parameters are only used when they are defined by crystal symmetry. An approximate (isotropic) treatment of cell esds is used for estimating esds involving l.s. planes.

Refinement. All hydrogen atoms were refined with standard riding models (d = 0.99 Å for methylene groups, d = 0.95 Å for aromatics) and $U_{iso}(H) = 1.2 \times U_{eq}(C)$.

Fractional atomic coordinates and isotropic or equivalent isotropic displacement parameters (Å^2)

	x	y	z	U_{iso}*/U_{eq}
C2	1.0441 (3)	0.65491 (8)	0.55310 (6)	0.0297 (3)
H2A	1.144473	0.699349	0.539126	0.036*
H2B	0.933591	0.672147	0.584572	0.036*
C3	0.8681 (3)	0.61985 (7)	0.50392 (6)	0.0284 (3)
H3A	0.979783	0.600009	0.473489	0.034*
H3B	0.760709	0.577146	0.518369	0.034*
C5	0.5116 (2)	0.66076 (7)	0.43693 (5)	0.0263 (3)
C6	0.4900 (3)	0.58992 (8)	0.41022 (6)	0.0296 (3)
H6	0.611055	0.549979	0.422126	0.036*
C7	0.2897 (3)	0.57723 (8)	0.36571 (6)	0.0330 (3)
H7	0.277119	0.528863	0.346947	0.040*
C8	0.1107 (3)	0.63442 (8)	0.34888 (6)	0.0333 (3)
H8	−0.026797	0.625078	0.319046	0.040*
C9	0.1303 (3)	0.70585 (8)	0.37543 (6)	0.0312 (3)
H9	0.006182	0.745160	0.363804	0.037*
C10	0.3313 (3)	0.71958 (7)	0.41884 (5)	0.0272 (3)
C12	0.1548 (3)	0.84138 (8)	0.44420 (6)	0.0354 (3)
H12A	−0.006134	0.817332	0.459237	0.042*
H12B	0.109109	0.857535	0.403608	0.042*
C13	0.2412 (3)	0.90949 (8)	0.48085 (6)	0.0400 (3)
H13A	0.406919	0.930919	0.465993	0.048*
H13B	0.099447	0.949141	0.475868	0.048*
C15	0.5467 (3)	0.85913 (10)	0.55533 (7)	0.0431 (4)

H15A	0.680158	0.878400	0.529116	0.052*
H15B	0.529938	0.803124	0.549722	0.052*
C16	0.6416 (3)	0.87554 (9)	0.61641 (7)	0.0418 (4)
H16A	0.833382	0.860914	0.623103	0.050*
H16B	0.626119	0.931038	0.624099	0.050*
C18	0.5696 (3)	0.84884 (9)	0.71328 (7)	0.0413 (3)
H18A	0.462399	0.891458	0.727912	0.050*
H18B	0.761253	0.864425	0.716177	0.050*
C19	0.5352 (3)	0.77915 (8)	0.74954 (6)	0.0343 (3)
H19A	0.558938	0.792103	0.791319	0.041*
H19B	0.353259	0.757138	0.741314	0.041*
C21	0.7615 (3)	0.66002 (7)	0.76567 (6)	0.0284 (3)
C22	0.6198 (3)	0.64255 (8)	0.81321 (6)	0.0326 (3)
H22	0.494445	0.678260	0.826614	0.039*
C23	0.6602 (3)	0.57274 (8)	0.84152 (6)	0.0362 (3)
H23	0.561808	0.561065	0.874138	0.043*
C24	0.8411 (3)	0.52054 (8)	0.82273 (6)	0.0363 (3)
H24	0.867921	0.473103	0.842373	0.044*
C25	0.9854 (3)	0.53739 (8)	0.77473 (6)	0.0329 (3)
H25	1.111404	0.501449	0.761901	0.039*
C26	0.9459 (2)	0.60618 (7)	0.74572 (6)	0.0283 (3)
C28	1.2710 (2)	0.57773 (8)	0.67757 (6)	0.0290 (3)
H28A	1.191303	0.527226	0.667225	0.035*
H28B	1.416418	0.570221	0.708571	0.035*
C29	1.3829 (3)	0.61383 (8)	0.62507 (6)	0.0316 (3)
H29A	1.390228	0.670029	0.630294	0.038*
H29B	1.568907	0.595295	0.621641	0.038*
O1	1.2240 (2)	0.59634 (6)	0.57316 (4)	0.0395 (3)
O4	0.69569 (18)	0.67957 (5)	0.48126 (4)	0.0302 (2)
O11	0.37362 (19)	0.78814 (5)	0.44656 (4)	0.0323 (2)
O14	0.2914 (2)	0.89471 (6)	0.54092 (4)	0.0422 (3)
O17	0.4851 (2)	0.83391 (6)	0.65474 (5)	0.0439 (3)
O20	0.7371 (2)	0.72584 (5)	0.73445 (4)	0.0354 (2)
O27	1.06917 (19)	0.62778 (5)	0.69739 (4)	0.0331 (2)

Atomic displacement parameters (Å²)

	U^{11}	U^{22}	U^{33}	U^{12}	U^{13}	U^{23}
C2	0.0276 (6)	0.0300 (7)	0.0313 (7)	0.0043 (5)	0.0006 (5)	−0.0009 (5)
C3	0.0262 (6)	0.0282 (6)	0.0304 (6)	0.0042 (5)	0.0004 (5)	−0.0001 (5)
C5	0.0219 (6)	0.0304 (6)	0.0266 (6)	0.0000 (5)	0.0025 (5)	−0.0008 (5)
C6	0.0249 (6)	0.0283 (6)	0.0357 (7)	0.0041 (5)	0.0018 (5)	−0.0027 (5)
C7	0.0302 (7)	0.0320 (7)	0.0365 (7)	−0.0008 (5)	0.0008 (5)	−0.0068 (6)
C8	0.0286 (7)	0.0388 (8)	0.0317 (7)	−0.0012 (5)	−0.0030 (5)	−0.0013 (6)
C9	0.0282 (7)	0.0329 (7)	0.0321 (7)	0.0039 (5)	0.0001 (5)	0.0042 (5)
C10	0.0281 (6)	0.0262 (6)	0.0278 (6)	0.0012 (5)	0.0054 (5)	−0.0002 (5)
C12	0.0371 (7)	0.0312 (7)	0.0378 (7)	0.0121 (6)	0.0031 (6)	0.0015 (6)
C13	0.0529 (9)	0.0323 (7)	0.0353 (7)	0.0120 (7)	0.0066 (6)	−0.0001 (6)

C15	0.0406 (8)	0.0492 (9)	0.0399 (8)	0.0075 (7)	0.0060 (6)	−0.0043 (7)
C16	0.0408 (8)	0.0411 (8)	0.0440 (8)	−0.0008 (6)	0.0056 (6)	−0.0073 (6)
C18	0.0532 (9)	0.0323 (7)	0.0377 (8)	0.0043 (7)	−0.0015 (7)	−0.0036 (6)
C19	0.0366 (7)	0.0316 (7)	0.0349 (7)	0.0064 (6)	0.0038 (6)	−0.0052 (6)
C21	0.0273 (6)	0.0262 (6)	0.0313 (6)	−0.0026 (5)	−0.0014 (5)	−0.0049 (5)
C22	0.0318 (7)	0.0317 (7)	0.0345 (7)	−0.0029 (5)	0.0041 (5)	−0.0071 (5)
C23	0.0376 (8)	0.0368 (8)	0.0344 (7)	−0.0071 (6)	0.0046 (6)	−0.0021 (6)
C24	0.0367 (7)	0.0310 (7)	0.0406 (8)	−0.0044 (6)	−0.0015 (6)	0.0026 (6)
C25	0.0278 (7)	0.0304 (7)	0.0400 (7)	0.0003 (5)	−0.0013 (5)	−0.0034 (6)
C26	0.0236 (6)	0.0303 (7)	0.0305 (6)	−0.0028 (5)	−0.0014 (5)	−0.0048 (5)
C28	0.0218 (6)	0.0309 (7)	0.0338 (7)	0.0037 (5)	−0.0015 (5)	−0.0061 (5)
C29	0.0270 (7)	0.0353 (7)	0.0320 (7)	0.0037 (5)	−0.0017 (5)	−0.0038 (5)
O1	0.0458 (6)	0.0367 (5)	0.0338 (5)	0.0139 (4)	−0.0116 (4)	−0.0084 (4)
O4	0.0272 (5)	0.0287 (5)	0.0338 (5)	0.0050 (4)	−0.0042 (4)	−0.0042 (4)
O11	0.0319 (5)	0.0267 (5)	0.0378 (5)	0.0061 (4)	−0.0005 (4)	−0.0043 (4)
O14	0.0436 (6)	0.0504 (6)	0.0335 (5)	0.0113 (5)	0.0078 (4)	−0.0021 (5)
O17	0.0525 (6)	0.0431 (6)	0.0355 (5)	−0.0040 (5)	−0.0007 (5)	0.0012 (4)
O20	0.0387 (5)	0.0302 (5)	0.0383 (5)	0.0064 (4)	0.0099 (4)	0.0006 (4)
O27	0.0310 (5)	0.0335 (5)	0.0353 (5)	0.0063 (4)	0.0068 (4)	−0.0003 (4)

Geometric parameters (Å, º)

C2—H2A	0.9900	C16—H16A	0.9900
C2—H2B	0.9900	C16—H16B	0.9900
C2—C3	1.5138 (18)	C16—O17	1.4214 (19)
C2—O1	1.4160 (16)	C18—H18A	0.9900
C3—H3A	0.9900	C18—H18B	0.9900
C3—H3B	0.9900	C18—C19	1.495 (2)
C3—O4	1.4267 (15)	C18—O17	1.4114 (18)
C5—C6	1.3841 (18)	C19—H19A	0.9900
C5—C10	1.4085 (18)	C19—H19B	0.9900
C5—O4	1.3646 (15)	C19—O20	1.4321 (16)
C6—H6	0.9500	C21—C22	1.3817 (19)
C6—C7	1.3977 (19)	C21—C26	1.4151 (18)
C7—H7	0.9500	C21—O20	1.3585 (16)
C7—C8	1.377 (2)	C22—H22	0.9500
C8—H8	0.9500	C22—C23	1.392 (2)
C8—C9	1.391 (2)	C23—H23	0.9500
C9—H9	0.9500	C23—C24	1.374 (2)
C9—C10	1.3858 (19)	C24—H24	0.9500
C10—O11	1.3678 (16)	C24—C25	1.395 (2)
C12—H12A	0.9900	C25—H25	0.9500
C12—H12B	0.9900	C25—C26	1.3834 (19)
C12—C13	1.505 (2)	C26—O27	1.3654 (16)
C12—O11	1.4308 (15)	C28—H28A	0.9900
C13—H13A	0.9900	C28—H28B	0.9900
C13—H13B	0.9900	C28—C29	1.5087 (19)
C13—O14	1.4159 (18)	C28—O27	1.4321 (15)

C15—H15A	0.9900	C29—H29A	0.9900
C15—H15B	0.9900	C29—H29B	0.9900
C15—C16	1.483 (2)	C29—O1	1.4216 (16)
C15—O14	1.4328 (19)		

H2A—C2—H2B	108.7	O17—C16—H16A	109.7
C3—C2—H2A	110.6	O17—C16—H16B	109.7
C3—C2—H2B	110.6	H18A—C18—H18B	108.1
O1—C2—H2A	110.6	C19—C18—H18A	109.6
O1—C2—H2B	110.6	C19—C18—H18B	109.6
O1—C2—C3	105.76 (10)	O17—C18—H18A	109.6
C2—C3—H3A	110.5	O17—C18—H18B	109.6
C2—C3—H3B	110.5	O17—C18—C19	110.35 (12)
H3A—C3—H3B	108.7	C18—C19—H19A	110.4
O4—C3—C2	106.26 (10)	C18—C19—H19B	110.4
O4—C3—H3A	110.5	H19A—C19—H19B	108.6
O4—C3—H3B	110.5	O20—C19—C18	106.42 (12)
C6—C5—C10	119.54 (12)	O20—C19—H19A	110.4
O4—C5—C6	125.21 (12)	O20—C19—H19B	110.4
O4—C5—C10	115.24 (11)	C22—C21—C26	119.51 (12)
C5—C6—H6	120.1	O20—C21—C22	125.29 (12)
C5—C6—C7	119.89 (12)	O20—C21—C26	115.20 (12)
C7—C6—H6	120.1	C21—C22—H22	119.9
C6—C7—H7	119.8	C21—C22—C23	120.14 (13)
C8—C7—C6	120.39 (13)	C23—C22—H22	119.9
C8—C7—H7	119.8	C22—C23—H23	119.7
C7—C8—H8	119.9	C24—C23—C22	120.62 (13)
C7—C8—C9	120.23 (12)	C24—C23—H23	119.7
C9—C8—H8	119.9	C23—C24—H24	120.1
C8—C9—H9	120.0	C23—C24—C25	119.86 (13)
C10—C9—C8	119.91 (12)	C25—C24—H24	120.1
C10—C9—H9	120.0	C24—C25—H25	119.8
C9—C10—C5	120.01 (12)	C26—C25—C24	120.31 (13)
O11—C10—C5	115.27 (11)	C26—C25—H25	119.8
O11—C10—C9	124.71 (12)	C25—C26—C21	119.55 (13)
H12A—C12—H12B	108.4	O27—C26—C21	115.01 (12)
C13—C12—H12A	110.1	O27—C26—C25	125.43 (12)
C13—C12—H12B	110.1	H28A—C28—H28B	108.4
O11—C12—H12A	110.1	C29—C28—H28A	110.1
O11—C12—H12B	110.1	C29—C28—H28B	110.1
O11—C12—C13	107.87 (12)	O27—C28—H28A	110.1
C12—C13—H13A	108.4	O27—C28—H28B	110.1
C12—C13—H13B	108.4	O27—C28—C29	108.05 (11)
H13A—C13—H13B	107.5	C28—C29—H29A	109.2
O14—C13—C12	115.47 (12)	C28—C29—H29B	109.2
O14—C13—H13A	108.4	H29A—C29—H29B	107.9
O14—C13—H13B	108.4	O1—C29—C28	111.89 (11)
H15A—C15—H15B	108.1	O1—C29—H29A	109.2

C16—C15—H15A	109.5	O1—C29—H29B	109.2
C16—C15—H15B	109.5	C2—O1—C29	114.92 (10)
O14—C15—H15A	109.5	C5—O4—C3	116.94 (10)
O14—C15—H15B	109.5	C10—O11—C12	117.42 (10)
O14—C15—C16	110.73 (12)	C13—O14—C15	113.46 (11)
C15—C16—H16A	109.7	C18—O17—C16	111.29 (12)
C15—C16—H16B	109.7	C21—O20—C19	117.34 (11)
H16A—C16—H16B	108.2	C26—O27—C28	117.35 (10)
O17—C16—C15	109.99 (13)		

C2—C3—O4—C5	−178.30 (10)	C22—C21—C26—O27	177.94 (11)
C3—C2—O1—C29	−171.31 (11)	C22—C21—O20—C19	−4.54 (19)
C5—C6—C7—C8	−1.1 (2)	C22—C23—C24—C25	−0.2 (2)
C5—C10—O11—C12	−160.54 (11)	C23—C24—C25—C26	−0.4 (2)
C6—C5—C10—C9	1.36 (19)	C24—C25—C26—C21	1.10 (19)
C6—C5—C10—O11	−178.08 (11)	C24—C25—C26—O27	−177.90 (12)
C6—C5—O4—C3	−3.98 (18)	C25—C26—O27—C28	−5.00 (18)
C6—C7—C8—C9	1.1 (2)	C26—C21—C22—C23	0.55 (19)
C7—C8—C9—C10	0.2 (2)	C26—C21—O20—C19	174.39 (11)
C8—C9—C10—C5	−1.4 (2)	C28—C29—O1—C2	100.04 (14)
C8—C9—C10—O11	177.99 (12)	C29—C28—O27—C26	−178.62 (10)
C9—C10—O11—C12	20.06 (18)	O1—C2—C3—O4	−176.91 (10)
C10—C5—C6—C7	−0.11 (19)	O4—C5—C6—C7	179.02 (12)
C10—C5—O4—C3	175.18 (11)	O4—C5—C10—C9	−177.86 (11)
C12—C13—O14—C15	78.08 (17)	O4—C5—C10—O11	2.71 (16)
C13—C12—O11—C10	176.07 (11)	O11—C12—C13—O14	−64.62 (16)
C15—C16—O17—C18	−179.56 (12)	O14—C15—C16—O17	72.03 (17)
C16—C15—O14—C13	155.01 (14)	O17—C18—C19—O20	71.48 (15)
C18—C19—O20—C21	174.35 (11)	O20—C21—C22—C23	179.43 (12)
C19—C18—O17—C16	−146.68 (13)	O20—C21—C26—C25	179.85 (11)
C21—C22—C23—C24	0.1 (2)	O20—C21—C26—O27	−1.05 (16)
C21—C26—O27—C28	175.96 (11)	O27—C28—C29—O1	−85.10 (13)
C22—C21—C26—C25	−1.16 (19)		

Hydrogen-bond geometry (Å, º)

D—H···*A*	*D*—H	H···*A*	*D*···*A*	*D*—H···*A*
C2—H2*A*···O11^{i}	0.99	2.94	3.8408 (17)	152
C6—H6···O1^{ii}	0.95	2.69	3.5630 (16)	154
C7—H7···O27^{iii}	0.95	3.36	4.2170 (17)	152
C13—H13*B*···O14^{iv}	0.99	3.36	4.3366 (18)	170
C16—H16*A*···O17^{i}	0.99	3.31	4.292 (2)	172
C19—H19*B*···O20^{v}	0.99	3.11	4.0729 (18)	165
C29—H29*A*···O17^{i}	0.99	2.95	3.9337 (18)	172
C29—H29*B*···O1^{i}	0.99	3.52	4.4497 (17)	156

Symmetry codes: (i) *x*+1, *y*, *z*; (ii) −*x*+2, −*y*+1, −*z*+1; (iii) −*x*+1, −*y*+1, −*z*+1; (iv) −*x*, −*y*+2, −*z*+1; (v) *x*−1, *y*, *z*.